CROSSINGS OF GEOSTATIONARY ORBIT BY THEMIS SCIENTIFIC SATELLITES

S. Frey [(1)] , M. Bester [(2)] , V. Angelopoulos [(3)]

[(1)(2)] *Space Sciences Laboratory, University of California, 7 Gauss Way, Berkeley, CA 94720-7450,*
(1) phone: 510-643-9880, email: sfrey@ssl.berkeley.edu,(2) phone: 510-643-1014, email: mbester@ssl.berkeley.edu
(3) ESS/IGPP, University of California, Los Angeles, 405 Hilgard Avenue, Los Angeles, CA 90095-1567
Phone: (310) 794-7090, Email: vassilis@ucla.edu

Abstract: *In this paper we outline how the argument of perigee can be used to determine the crossings of a geosynchronous orbit through the geostationary orbit without any extensive computational efforts. The peculiarity of this geometry is that the semi-major axis of any geosynchronous orbit equals the geostationary distance and by definition any geosynchronous spacecraft crossing the geostationary orbit is either at the ascending or the descending node. Using standard equations of satellite motion we show that the eccentric anomaly is 90 degrees at that moment, and the true anomaly is only defined by the eccentricity of the geostationary orbit. We illustrate, that for any given eccentricity there are four values for the argument of perigee at which the spacecraft crosses the equatorial plane at geostationary distance.*

Keywords: THEMIS mission, multi-spacecraft mission, geosynchronous orbit, geostationary orbit.

1. Introduction

Since February 2007 NASA's multi-spacecraft Time History of Events and Macroscale Interactions during Substorms (**THEMIS**) mission has been successfully collecting high time resolution data of plasma particles and electromagnetic fields in the Earth's magnetosphere [1]. At the center of the scientific research are the magnetospheric processes leading up to substorm onsets that are visible to us through the dynamic outbreaks of bright polar lights. During the two year nominal mission the five identical probes were kept on synchronized, highly elliptical, and nearly equatorial orbits with periods of 4, 2, 1, 1, and 1 days to form large scale conjunctions in the magnetospheric tail every 4 days. Since 2009 the mission has been split into two extended

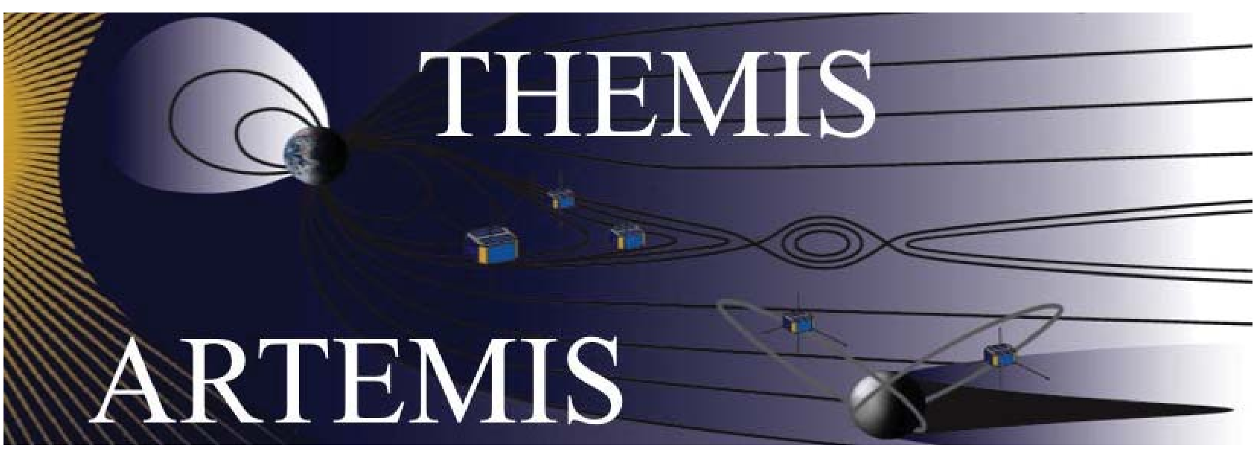

Figure 1. Logo of the extended mission, an artist's rendering of the magnetospheric tail configuration with Moon, THEMIS, and ARTEMIS satellites opposing the Sun's direction

missions. The two outer probes have been brought into lunar orbits and have been renamed as Acceleration, Reconnection, Turbulence and Electrodynamics of the Moon's Interaction with the Sun (**ARTEMIS**). After a challenging journey through lunar libration orbits lunar science orbits started in summer 2011 [2]. At the start of 2010, the remaining three near-Earth THEMIS probes have been brought into a smaller formation on low Earth geosynchronous orbits to address different questions about magnetospheric processes on smaller scales. Figure 1 illustrates, not to scale, the magnetospheric tail configuration with the Moon, THEMIS and ARTEMIS satellites. The topography of the Earth's magnetosphere, shaded in blue, is visualized by magnetic field lines. The ARTEMIS probes are captured on their lunar orbits at the moment when one probe is entering the Moon's plasma wake, while the THEMIS probes are placed near 11 Earth radii to monitor the disruption of the dipole field structures. Thanks to sufficient fuel reserves and our ability to actively alter the orbits we are able to significantly vary orbit shape and orientation with regards to the equatorial plane twice per year. These orbit redesigns are guided by the feedback from the most recent findings from our science data.

THEMIS and its extended missions are managed in PI mode by U.C. Berkeley. Mission operations and science data processing are highly automated allowing our relatively small multi-mission operations team to handle all flight and ground systems operations such as S/C commanding, data retrieval, and processing, as well as mission design and navigation very efficiently [3]. With the THEMIS satellites in orbit now for over 5 years we gained a lot of experience in navigating and operating satellites in highly elliptical orbits in the Earth and lunar environment [4, 5, 6]. In this paper we focus on our analysis of the low Earth geosynchronous orbits and their intersections with the geostationary orbit.

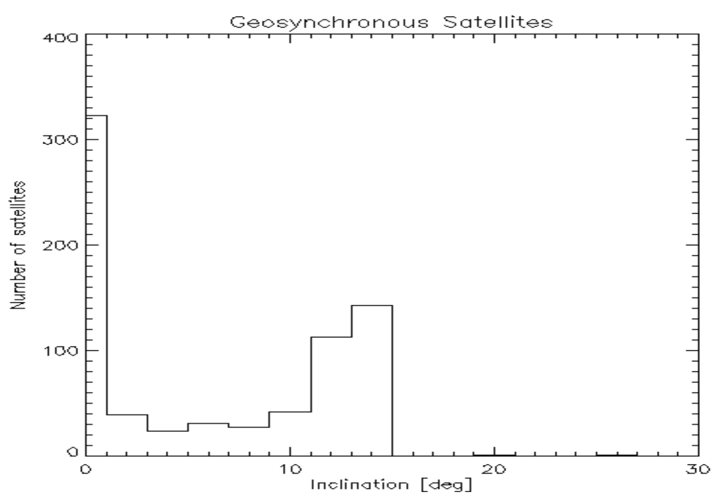

Figure 2. Distribution of geostationary satellites by inclination.

In the first year of the extended mission phase the three THEMIS satellites were reaching very low inclinations having dropped from 7 to 1 degree, raising concerns about close encounters with objects in geostationary orbits. Figure 2 shows the distribution of the ~800 publicly known geostationary satellites as a function of inclination and underlines that low inclination orbits are the most populated ones. As we were facing an increasing probability of close encounters with geostationary objects we were interested in routinely predicting these equatorial crossings and furthermore investigating the effect of our frequent orbit refinements on the number and timing of such crossings. As the number of space objects, particularly in the geostationary orbit, is growing at a high rate we believe that this study is of general interest to the space flight community.

It is not the paper's purpose to present a detailed assessment of conjunctions with geostationary objects. Nor would we have knowledge of a comprehensive list of all such objects. Our intent is to determine the driving orbital parameters and to develop a method to predict crossings of geostationary orbits from THEMIS orbit data that can be integrated into our mission design and operational routines [7]. First we will analytically show that the argument of perigee can be used to determine the crossings of a geosynchronous orbit through the geostationary orbit without any extensive computational efforts and evaluate the effect of small changes of the geosynchronous orbit. For long-term predictions of crossings we will demonstrate the need of a high fidelity orbit propagator especially at low inclinations. Second, we will empirically analyze crossings of THEMIS orbits through a small belt of geostationary orbits. Third, we will illustrate the effect of inclination on those crossings. Finally and last, we will summarize our findings and outline the operational benefits. Though this analysis has been done with THEMIS data and within a parameter range confined by the THEMIS orbits the outlined method and trends are of general nature and the parameter space can easily be extended.

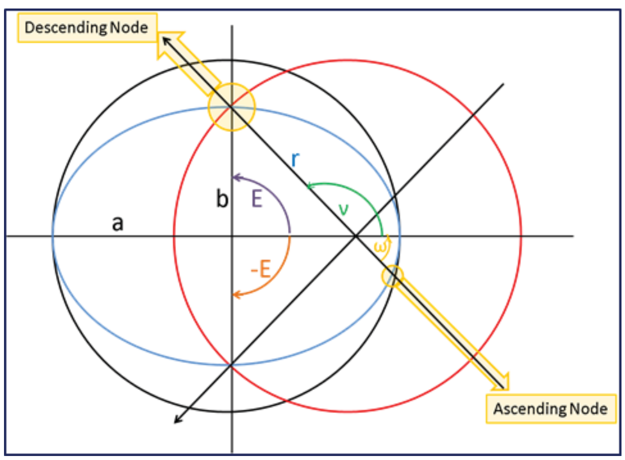

Figure 3. Intersection of a geosynchronous orbit (blue) and the geostationary orbit (red), not to scale. Keplerian elements are indicated for a spacecraft in the geosynchronous orbit at the descending node.

2. The Argument of Perigee as a Parameter to Identify Crossings of Geosynchronous Orbits through the Equatorial Geostationary Orbit

2.1. Analytical Approach

At first we reduce the multiple trajectory problem into one of two orbits by replacing individual orbits of geostationary objects by the equatorial geostationary orbit and the highly elliptical THEMIS orbits which differ slightly in altitudes and inclination by an equatorial geosynchronous orbit. The extracted geometry between geostationary and geosynchronous orbits in the equatorial plane is shown in Fig. 3 and we can easily apply standard equations of satellite motion [8]. When in the same plane both orbits always intersect at two points. At either intersection the distance to the primary focus **r** is the same for both orbits and equals the geostationary distance. By definition the semi-major axis **a** of the geosynchronous orbit equals the geostationary distance. If we apply a=r to the definition of the distance to the primary focus (Eq. 1), we get the eccentric anomaly **E**=90 degrees and according to Eq. 2 the true anomaly **ν** is only defined by the eccentricity **e**, as Eq. 3 shows, where $\mathbf{r_p}$ is the geocentric perigee altitude.

$$r = a(1 - e * \cos(E)) \quad (1)$$

$$\cos(\nu) = \frac{\cos(E) - e}{1 - e * cos(E)} \quad (2)$$

$$\cos(\boldsymbol{\nu}) = -\mathbf{e} \quad (3)$$

$$e = 1 - \frac{r_p}{a} \quad (4)$$

Applying the symmetry of the cosine function, Eq. 3 provides the true anomaly for the two intersections as:

$$\nu_1 = |\nu| \quad (5a)$$

$$\nu_2 = -|\nu| \quad (5b)$$

From Kepler's equation, Eq. 6, we obtain the mean anomaly **M**. Knowing the eccentricity we can define the true and mean anomalies of the intersections.

$$M = E - e * \sin(E) \quad (6)$$

If the inclination of the geosynchronous orbit is non-zero both orbits in Fig. 3 intersect at the distant node where r=a. Since the true anomaly is defined from perigee in the direction of the S/C and the argument of perigee $\boldsymbol{\omega}$ is defined from the ascending node in the direction of the S/C we can determine the argument of perigee at the ascending node $\boldsymbol{\omega_A}$ and descending $\boldsymbol{\omega_D}$ node by Equations 7a and 7b.

$$\omega_A = 360 - \nu \quad (7a)$$

$$\omega_D = \omega_A - 180 \quad (7b)$$

Since both angles, true anomaly and argument of perigee, are defined in the orbital plane, the results of Eq. 7a and 7b are independent from the inclination. Hence, for any given eccentricity of the geosynchronous orbit we get four values for the argument of perigee, one per quadrant, at which the S/C cross the equatorial plane at geostationary distance. Just knowing in what quadrant the argument of perigee falls we can characterize the crossing, whether it is ascending or descending and inbound, E=-90 deg, or outbound, E=90 deg, using Tab. 1.

Table 1. Critical Argument of perigees and their location

Quadrant	I	II	III	IV
Location	outbound	inbound	outbound	inbound
Node	descending	ascending	ascending	descending
ω [deg]	40	140	220	320

On geosynchronous orbits, where the semi-major axis is constant, we determine the argument of perigee from perigee altitude alone using Eq. 4. Figure 4 shows the arguments of perigee at the crossings for perigee altitudes between 600 and 4350 km. Over this wide range the argument of perigee changes only by 5 degrees, and we can use the values for ω in Tab. 1 as representative mean values to make long term predictions.

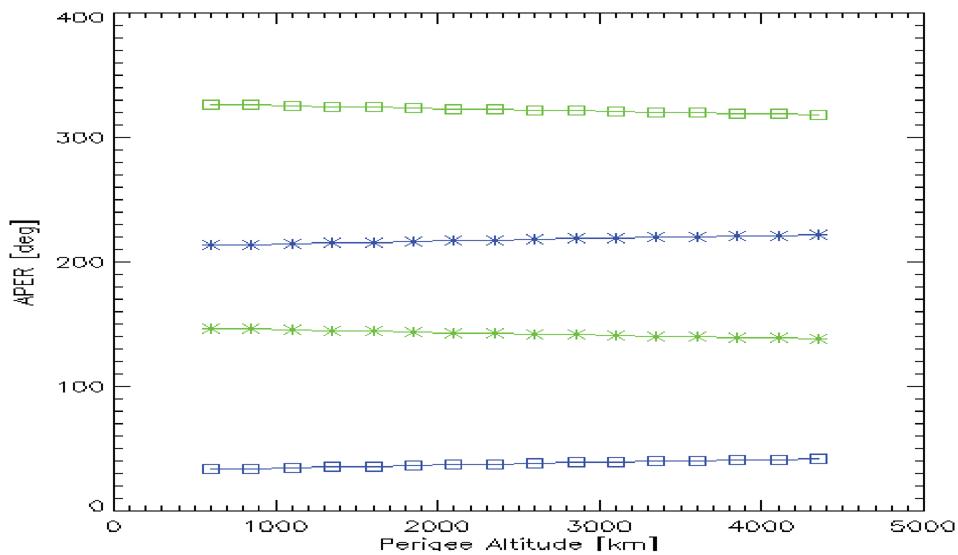

Figure 4: Argument of perigee in degrees of a geosynchronous orbit at crossings through the geostationary orbit as function of perigee altitude in km. Green refers to inbound, blue to outbound, stars mark ascending nodes, squares mark descending nodes.

Were it not for orbit perturbations such as the non-uniform mass distribution of Earth, and the presence of the Sun and Moon the orbits would not rotate and we could avoid any critical orientation of our line of nodes. But if we stay long enough in orbit we will pass over each one of the four critical arguments of perigee multiple times and become interested in long term predictions based on the change rate of the argument of perigee. The main contribution to the change rate of the argument of perigee comes from the Earth's oblateness (J2-term) making it a function of inclination and eccentricity, for which we have well defined analytical expressions [8]. Whereas solar-lunar effects on the inclination at geostationary distances and on the even higher geosynchronous orbits are much smaller but yet significant. Figure 5 shows how misleading

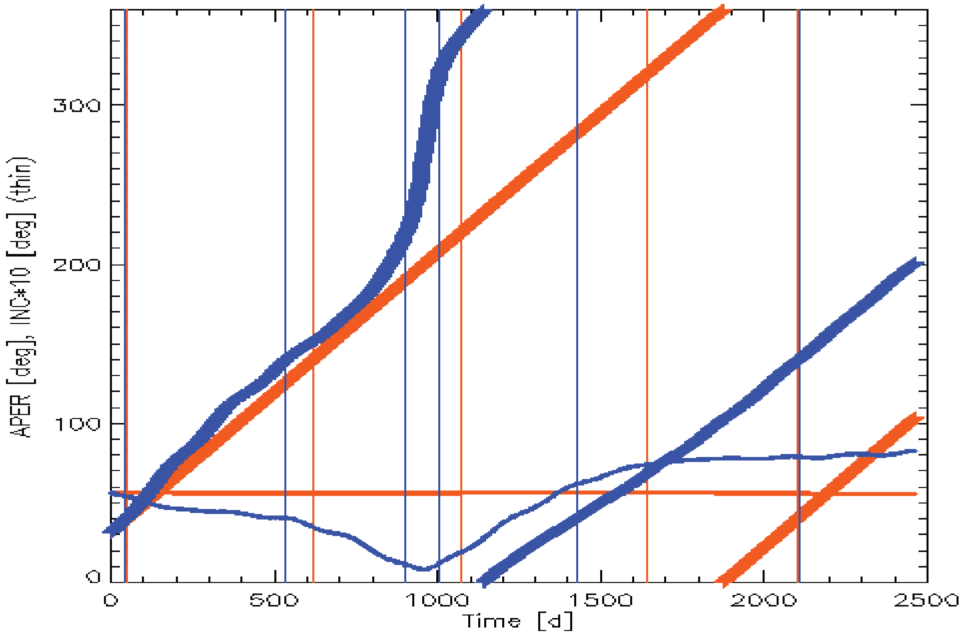

Figure 5: Comparing the evolution of the argument of perigee (thick) and inclination*10 (thin) in degrees from April 2008 to December 2014, based on Earth oblateness only (red) and with solar-lunar perturbations included (blue). Initial perigee altitude is 2818 km. Time is in days.

it can be to solely rely on Earth's contribution to orbit perturbations for long term predictions. In Fig. 5 we compare the evolution of the argument of perigee for a THEMIS orbit over nearly 7 years based on J2-perturbation only, with those that have solar and lunar perturbation included. We see that deviations of the times the orbit reaches a critical argument of perigee for crossings increase rapidly. Once the orbital plane is being pulled down the change rate of the argument of perigee increases and is not a monotone function of time any more. Table 2 compares the duration from one critical argument of perigee to the next for the two perturbation models in Fig. 5. The shift in crossing times between the two models, shown in the last column grows quickly from a few days to almost two years in the course of one node revolution. Since the orbits actually rotate faster, the crossings happen earlier, which can lead to unwelcome surprises. Hence, for reliable long term prediction of crossing times it is important to use a high fidelity orbit propagator such the Goddard Trajectory Determination System, GTDS [9].

Table 2: Critical argument of perigee and change rates according to Fig.5

ω [deg]	40	140	220	320	40	140
Inc. [deg]	5.5	4.0	1.3	1.5	7.0	8.0
$\Delta\omega$ [deg]	-	100	80	100	80	100
Δt_1 [d]	-	565	460	565	460	565
Δt_2 [d]	-	490	368	104	419	680
Δt_{21}[d]	-6	-83	-170	-637	-676	-550

The implication of Eq. 3 is that as long as we are at or near the geosynchronous orbital period there is no way of avoiding crossings of the geostationary orbit. Varying the perigee altitude of the geosynchronous orbit will only shift the intersection along the orbit which may help temporarily. For short missions and given flexibility in choosing the initial argument of perigee one can place the mission into the longer periods between crossings.

2.2. Empirical Approach

In our empirical approach we go back to the multiple trajectory problem and extend the geostationary orbit by a belt that is centered at the equatorial geostationary distance and defined by a range in the radial distance Δ**r** and in the geocentric equatorial Z-component Δ**z**. In selecting Δr and particularly Δz we wanted to take into account the inclination range of geostationary orbits as shown in Fig. 2 In a second, more restricted survey of geostationary objects as a function of inclination with SatTrack [10], confining inclination to less than 1 degree, eccentricity within 0-0.05, and period within 1430 to 1450 min, we found 90% of those objects to be within .1 degrees of inclination. Based on these results, listed in Tab. 3, we chose $\Delta r=\pm150$ km and $\Delta z=\pm100$ km and determined the intersecting arcs of the THEMIS orbits, using high fidelity ephemeris at high time resolution. As crossing time per orbit we take the time of the minima of Δr and Δz along each arc inside the window. The results are visualized as time series of argument of perigee and inclination in Fig. 6, as well as orbit tracks in the Δr - Δz window in Fig 7. In Fig. 6 the vertical lines mark the time of crossings and intersect the argument of perigee curve around the predicted critical values for argument of perigee as in Tab. 1. The thicker these lines appear the more crossings we find around a particular argument of perigee, which we call a crossing season. The length of a season is driven by the change rate of the argument of perigee. Figure 7 shows not only how the consecutive orbits per season step through the Δz range according to the inclination but also characterizes how the probe approaches the geostationary orbit.

Table 3: Geostationary object counts for very low inclination ranges and corresponding dz in km at geostationary distance.

Inc. [deg]	.025	0.05	0.1	0.5	0.8
|dz| [km]	18	37	74	368	589
object count	109	186	250	267	278

With Fig. 6 and Tab. 1 we can easily interpret Fig. 7 where inbound legs move from right to left. In 2011, the 7 crossings (blue) happen at the descending node on the inbound leg which means an approach from above and outside the geostationary belt. Due to an inclination of only 3.5 degrees, orbits occupy only the center part of the Δz range. In 2012, 16 crossings (cyan) happen at the descending node on the outbound leg at inclination 9.5 degrees. In 2014, the 11 (green) crossings happen at the ascending node at an inclination of 11 degrees. Knowing this information may be helpful in guiding what action should be taken in case of a close encounter.

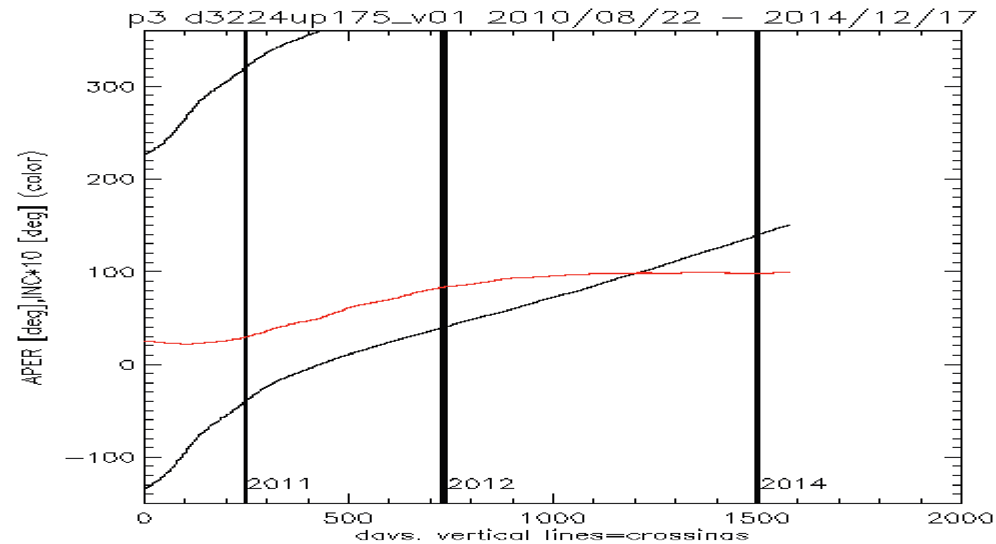

Figure 6: Argument of perigee of a THEMIS probe (black) and inclination (red) , enhanced by a factor 10 in degree, August 2010 to December 2014, based on high fidelity orbit propagation without maneuvers. Vertical lines are crossings of probe through the belt centered at geostationary orbit. Initial perigee altitude is 3794 km.

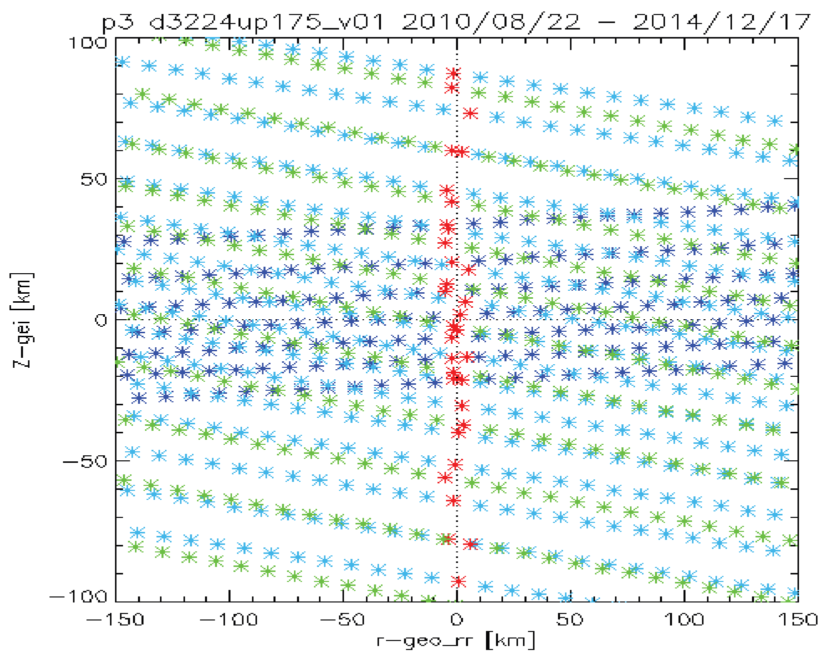

Figure 7: Orbit tracks of same data as in Fig. 6 relative to equatorial geostationary orbit. Colors refer to vertical lines in Fig. 6 as blue: 2011, cyan: 2012, green: 2014.

2.3. The Effect of Inclination

While the argument of perigee defines the condition for crossings the inclination defines the geometry and thus density of crossings per season. The lower the inclination the more tangential the geosynchronous and geostationary orbits become narrowing the Δz range but stretching the critical along-track range. Orbits with higher inclinations are more separated in z which shortens the critical along-track range. Thus for our purposes in this analysis the perturbing interactions of Earth, Sun, and Moon on the nodes are best referenced by inclination although the change rate of the argument of perigee also depends on perigee altitude at a given apogee altitude. In order to analyze how inclination effects the crossings we repeated the high fidelity propagation of the THEMIS orbit from April 2008, as used in Fig. 5, at higher inclinations. In Figure 8 we compare the change of the rotation rates for the different initial inclinations.

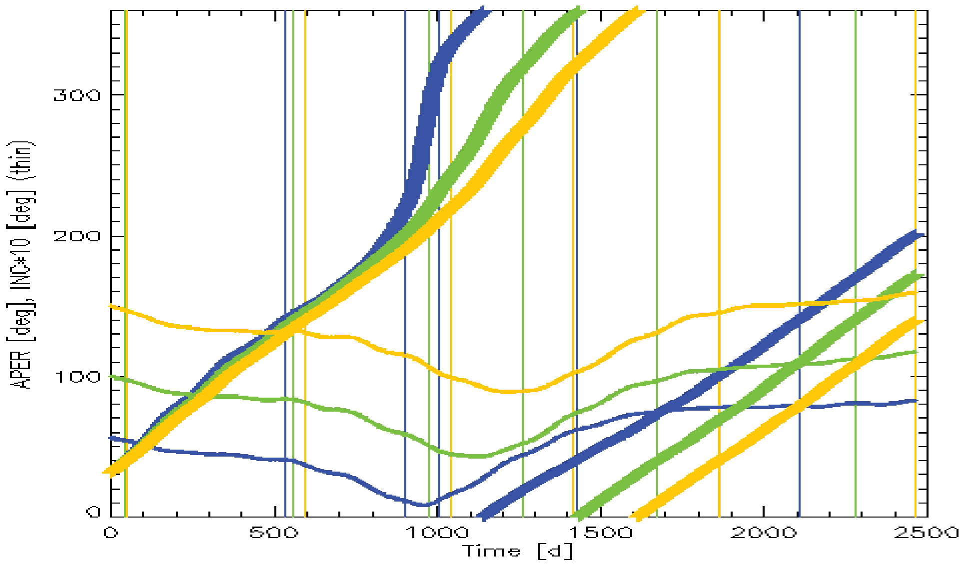

Figure 8: Argument of perigee of a THEMIS probe (thick) and inclination (thin), enhanced by factor 10, between April 2008 and December 2014 based on high fidelity orbit simulations. Colors indicate different inclinations as blue 5.5 deg, green 10 deg, and yellow 15 deg.

For each orbit at very low inclinations the change rate of argument of perigee is higher causing fewer crossings per season but also leading into the next crossing season much faster. Furthermore, Fig. 8 shows that the most drastic change rate of argument of perigee and thus the timing of crossings, happens around the orbital minimum inclination. These minima always fall between the crossings at ω=220 deg and ω=320 deg for any inclination in the analyzed range. The lower the initial inclination the stronger this trend is. In a last step we repeated the analysis and reduced perigee altitudes from 2818 km by 1000km at the highest and lowest inclinations shown in Fig. 8. Not surprisingly by increasing inclination and/or perigee altitude we can delay crossings. However, since inclination and perigee altitude are also changing due to perturbations depending on argument of perigee changing perigee altitude can be more effective than changing inclination and vice versa as Fig. 9 illustrates.

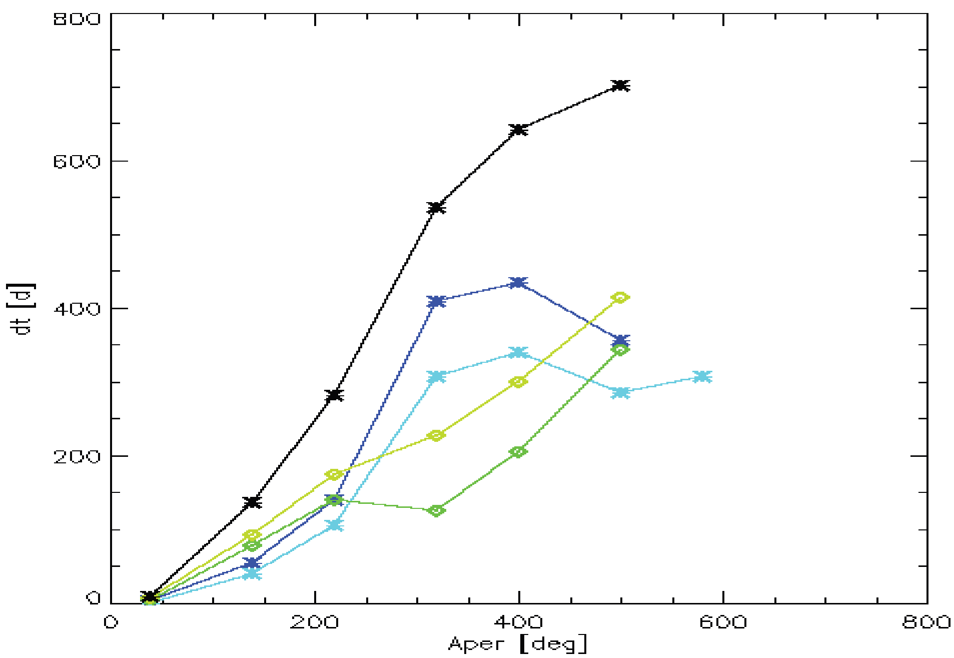

Figure 9: Accumulated time offsets at reaching critical arguments of perigee due to change in inclination and/or perigee altitude. Black-increasing inclination and perigee altitude, green hues-increase of perigee at low (dark) and high (light) inclination, blue hues-increase of inclination at low (light) and high (dark) perigee altitude. Low inclination 5.5, high inclination 15 degrees. Low perigee 1818 km, high perigee 2818 km.

3. Conclusions

3.1 Implications for THEMIS orbit design and operations

A satellite in a geosynchronous orbit will always rotate through the four critical values of argument of perigee and cross the geostationary orbit. Once in orbit options to temporarily modify such crossings through orbit design are limited to changing the event times and the geographic longitudes by selecting perigee or/and inclination. Both modifications are costly in dV, alone changing perigee by 250 km takes about 18 m/s. For us this is too large a maneuver that may reduce a potential risk only temporarily. For short missions of one or two years, the choice of initial inclination and argument of perigee can be selected such as to avoid crossings during nominal mission lifetime, at least at very low inclinations if that does not interfere with primary mission requirements.

For THEMIS the decision has been made to monitor crossing seasons routinely. Our frequent orbit redesigns alter perigee and respectively apogee altitudes in the order of a few tens to thousands of kilometers, which can quickly move an upcoming crossing season back or forth by days or weeks. In order to make this analysis suitable for our automated mission design and weekly checkups of updated ephemeris we first determine from long term high fidelity data at low time resolution the times of passing through the critical values of argument of perigee. If such instances are found high time resolution data are automatically generated around those events and analyzed as shown in Figures 6 and 7 and the center times of the crossings are listed in the report file.

3.2 Summary

We have shown that for any given eccentricity there are four values for the argument of perigee at which the geosynchronous spacecraft cross the equatorial plane at geostationary distance.
We have demonstrated that we can predict crossings of the geosynchronous orbit through a geostationary belt with very little computational effort and without the need of an extensive database. That enables us to integrate it in our routine mission operations and orbit designs.
Having the long-term knowledge of potential encounters with geostationary objects has been proven to be very beneficial for our long term operations planning. It prevents surprises. We are well aware that there can be close conjunctions with objects in other orbits. However, knowing as much as possible about such events is part of our risk mitigation strategy.

7. Acknowledgments

The THEMIS and ARTEMIS missions are operated by the University of California, Berkeley Space Sciences Laboratory under NASA contract NAS5-02099.

8. References

[1] Burch J.L. and Angelopoulos V., The THEMIS Mission, Space Science Reviews, Vol. 141, Issues 1-4, 2008.
[2] Angelopoulos, V. , The ARTEMIS Mission, Space Science Reviews, Vol. 165, Issue 5,2011
[3] Bester, M., Lewis, M., Roberts, B., Thorsness, J., McDonald, J., Pease, D., Frey, S., and Cosgrove, D., “Multi-mission Flight Operations at UC Berkeley – Experiences and Lessons Learned,” Proceedings of the AIAA 2010 SpaceOps Conference, Huntsville, AL, Apr. 25-30, 2010.
[4] Cosgrove, D., Frey, S., Marchese, J., Owens, B., and Bester, M., (2012), "ARTEMIS Operations from Earth-Moon Libration Orbits to Stable Lunar Orbits," Proceedings of the 12th International Conference on Space Operations (SpaceOps 2012), Jun. 11-15, Stockholm, Sweden.
[5] Marchese, J. E.; D. Cosgrove; M. Woodard; D. Folta; P. Morinelli; B. D. Owens; S. Frey; and M. G. Bester (2012), "Optimizing Solar Radiation Coefficient as a Solve-For Parameter for the Orbit Determination Process During the Libration-Point Orbit Phase of the ARTEMIS Mission," Proceedings of the 22nd AAS/AIAA Space Flight Mechanics Meeting, Charleston, SC, Jan. 29-Feb. 2, 2012; AAS 12-183.
[6] Frey S., M. Bester, V. Angelopoulos, Alignment of the THEMIS low extended mission with the magnetospheric neutral sheet, Proceedings 22nd International Symposium on Space Flight Dynamics – 22nd ISSFD, São José dos Campos, SP, Brazil, from February 28 to March 4, 2011.
[7] Frey S. et al. THEMIS: Implementation of a Challenging Missions Design, Proceedings 21th International Symposium on Space Flight Dynamics – 21th ISSFD, Toulouse, France, 2009.
[8] Vallado, D.A. Fundamentals of Astronomics and Applications, Space Technology Series, The McGraw-Hill Companies, Inc., College Custom Series, 1997
[9] GTDS, Goddard Trajectory Determination System, Software Package, Ver. 2003.01, NASA Goddard Space Flight Center, Greenbelt, MD, 2003
[10] SatTrack, Satellite Tracking and Orbit Analysis Software Suite, Software Package, Ver. 4.12.1, BTS, Richmond, CA,2012